

## Glycerol and Ethanol Oxidation in Alkaline Medium Using PtCu/C Electrocatalysts

C.A. Ottoni<sup>1</sup>, C.E.D. Ramos<sup>2</sup>, R.F.B. de Souza<sup>3</sup>, S.G. da Silva<sup>2</sup>, E.V. Spinace<sup>2</sup> and A.O. Neto<sup>2\*</sup>

<sup>1</sup> Bioscience Institute, São Paulo State University, 11380-972 São Vicente, SP, Brazil.

<sup>2</sup> Instituto de Pesquisas Energéticas e Nucleares, IPEN/CNEN-SP, Av. Prof. Lineu Prestes, 2242 Cidade Universitária, CEP 05508-900 São Paulo, SP, Brazil.

<sup>3</sup> Department of Chemistry, Federal University of Amazonas, Av. General Rodrigo Octávio, 6200, Coroado I CEP: 69080-900, Manaus, AM, Brazil.

\*E-mail: [aolivei@ipen.br](mailto:aolivei@ipen.br)

*Received:* 25 June 2017 / *Accepted:* 13 December 2017 / *Published:* 28 December 2017

---

The performance of platinum-copper electrocatalysts synthesized in different ratios (100:0, 90:10, 70:30, 50:50, and 0:100), using a borohydride reduction method for electrochemical oxidation of different fuels, was evaluated in an alkaline direct alcohol fuel cell. X-ray diffraction of Pt/C and PtCu/C showed a face-centered cubic structure (fcc) of the platinum and its alloys. Transmission electron microscopy analysis allowed us to see a good dispersion of metallic particles with some regions with clusters of nanoparticles, for all the synthesised materials in the presence of copper. Cyclic voltammetry and chronoamperometry tests demonstrated that the PtCu/C (50:50) and PtCu/C (70:30) electrocatalysts exhibited the highest activity and stability for the glycerol and ethanol oxidation, respectively. The tests made in fuel cells, directly fed with glycerol and ethanol, presented the PtCu/C (90:10) electrocatalyst as the most effective on the oxidation reaction of the fuels when compared with Pt/C and Cu/C.

---

**Keywords:** Direct ethanol fuel cell, direct glycerol fuel cell, PtCu electrocatalysts, alkaline fuel cell

### 1. INTRODUCTION

The increase in world demand of energy and related environmental concerns have been catalysing the research on energy sources with high efficiency of energetic conversion and low emissions of pollutants. The fuel cell technology is one of the most studied fields on renewable energy for producing relatively "clean" energy and high density of potency [1].

Direct alkaline alcohol fuel cells (DAAFCs) using liquid fuels such as methanol, ethanol, ethylene glycol, glycerol [2,3] have attracted attention of many researchers around the globe for having multiple advantages, especially when compared with hydrogen gas [4]. Ethanol has much lower toxicity than methanol [5], and glycerol, has been a very attractive choice due to: its low toxicity, its high energy density, be less susceptible to crossover, and be relatively inexpensive [6]. The challenge for utilizing glycerol in fuel cells is that the electrocatalytic oxidation of glycerol requires higher overpotentials to achieve a suitable current. To overcome this issue new electrocatalysts (EC) for glycerol oxidation have been developed [7].

Several studies have been conducted using different noble and transition metals on the EC composition to improve the direct glycerol fuel cell (DGFC) performance under alkaline condition [8-10]. Platinum (Pt) and its alloys are the most commonly EC applied on the anode, for their stability and high chemical activity [11]. Copper (Cu) has been combined with Pt to form low cost alloys, improving catalytic properties towards ethanol [12], formic acid [13] and methanol [14] oxidation.

Rezaei [15] prepared a modified Cu filled nanoporous stainless steel (NPSS) electrode as support for Pt and Pd (Pt-Pd/Cu/NPSS), for glycerol electro-oxidation in alkaline condition. Pt-Pd/Cu/NPSS electrode, with the Pt:Pd atomic ratio of 1:2 on the surface, exhibits high activity for electrocatalytic oxidation of glycerol. Munoz [16] demonstrated that Pd<sub>87</sub>Cu<sub>13</sub>/C was the most efficient EC, when compared with Pd/C, for the electrochemical oxidation of ethylene glycol, propylene glycol, and glycerol in alkaline media. These are due to contributions from the bifunctional and electronic effect, with the most significant contributions likely coming from the bifunctional effects. However, there is no known description in literature of PtCu/C EC application for glycerol oxidation under alkaline conditions.

In this context, the aim of this work was to prepare Pt/C and Pt/Cu electrocatalysts, in different ratios, by borohydride reduction method, and to test them for glycerol and ethanol electro-oxidation in alkaline medium through: cyclic voltammetry, chronoamperometry and in a DAAFC.

## 2. MATERIAL AND METHODS

Pt/C, PtCu/C (90:10, 70:30, 50:50), Cu/C electrocatalysts, all with 20% of mass of nominal metal filler, were prepared by the sodium borohydride reduction method [17, 18]. For these synthesis, several salts were used, platinum (H<sub>2</sub>PtCl<sub>6</sub>.6H<sub>2</sub>O, Aldrich) and copper (CuSO<sub>4</sub>, Aldrich), as precursors of metals and Vulcan XC72 carbon used as support. The support was added in a mixture containing a water/2-propanol (50:50 v/v) solution and precursor salts. The resulting mixture was subjected to the ultrasonic treatment for 10 minutes. After this step, a solution of sodium borohydride (NaBH<sub>4</sub>) diluted in 0.01 mol L<sup>-1</sup> NaOH was added and kept under mechanical stirring for 30 minutes at room temperature. Finally, the mixture was vacuum filtered and the solid part (electrocatalyst) obtained was washed with deionized water (ultrapure) and dried in the incubator at 70 °C for 2 hours.

The electrocatalysts were characterized morphologically by X-ray diffraction (XRD) and transmission electron microscopy (TEM). The X-ray diffraction measurements were obtained in a conventional Rigaku diffractometer (MiniFlex II model), using a CuK $\alpha$  radiation source ( $\lambda = 1.54056$

Å). The experiments were performed at  $2\theta$  in the scanning range of  $20^\circ$  to  $90^\circ$  with a scan speed of  $2^\circ$  ( $2\theta$ )/min. A JEOL electronic microscope (model JEM-2100) operated at 200 kV was used for TEM analysis. The average nanoparticle sizes were measured by counting approximately 100 nanoparticles in different regions of each sample, which were then used for the construction of histograms and determination of the average size of the nanoparticles.

The electrochemical profiles and electrocatalytic activities of the electrocatalysts were evaluated by cyclic voltammetry and chronoamperometry experiments. The electrochemical studies were carried out in an electrochemical cell of one compartment, with the electrocatalyst being used as the working electrode (geometric area of  $0.3\text{ cm}^2$ , with a depth of 0.3 mm) prepared using the porous thin layer technique. The porous thin layer technique consists of the preparation of a paste, done by mixing 20 mg of electrocatalyst, 50 mL of ultrapure water and 3 drops of a 6% (v/v) Teflon® - polytetrafluoroethylene (PTFE) dispersion.

The resulting mixture was subjected to ultrasonic agitation for 10 minutes. Subsequently, that mixture was filtered and the solid part was adhered to the cavity of the working electrode (0.3 mm depth) still wet, and then compacted in a way that allowed for the surface to be homogeneous. The reversible hydrogen electrode (RHE) and the Ag/AgCl electrode ( $3\text{ mol L}^{-1}$  KCl) were used as reference electrodes and a platinum plate as a counterelectrode. The cyclic voltammetry analyses were conducted at a scan rate of  $10\text{ mVs}^{-1}$  in KOH ( $1\text{ mol L}^{-1}$ ) in the presence and absence of glycerol or ethanol ( $1\text{ mol L}^{-1}$ ), while that of chronoamperometry (amperometric curves) were recorded in the same electrolyte containing glycerol at  $-0.35\text{ V}$  for 1800 s. All measurements were conducted at room temperature [19].

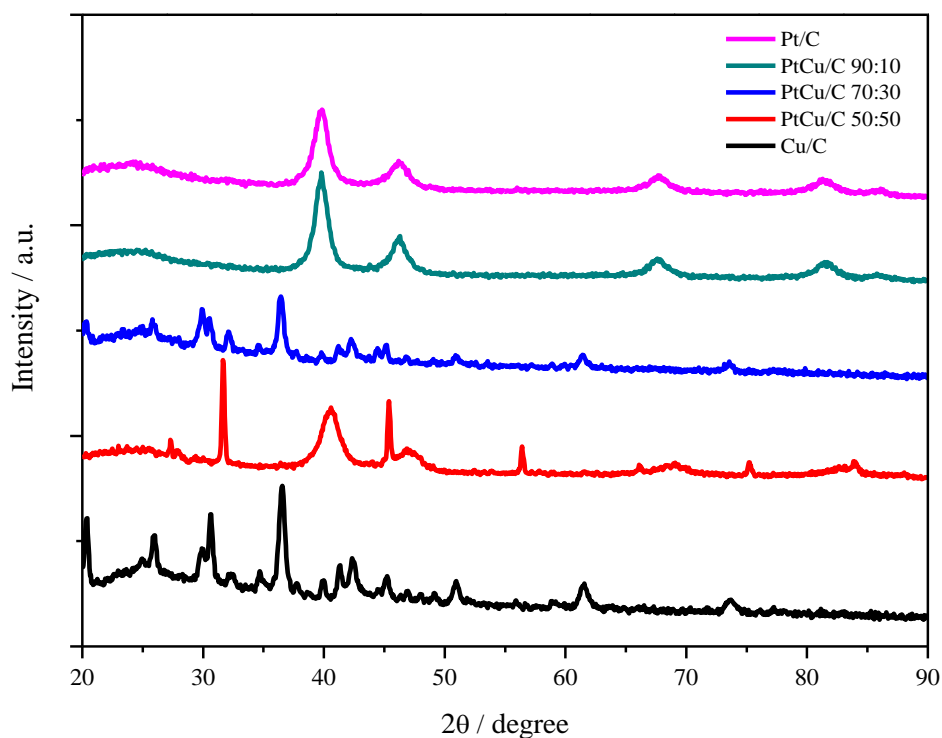
The following electrocatalysts: Pt/C, PtCu/C (90:10; 70:30; 50:50) or Cu/C electrocatalysts were used as anodes in order to study direct alkaline glycerol/ethanol fuel cells. For a single cell with an area of  $5\text{ cm}^2$ ,  $2\text{ mg}_{\text{Pt}}\text{ cm}^2$  and Nafion® 30% (5%, wt, Aldrich), were used for each electrocatalyst. For all the other cathodes Pt/C (BASF) electrocatalysts,  $2\text{ mg}_{\text{Pt}}\text{ cm}^2$  and Nafion® 30% were applied. All the electrocatalysts in the form of a homogeneous dispersion prepared using Nafion solution (5 wt%, Aldrich), were painted over a carbon cloth. The anode and cathode were hot pressed on both sides of a Nafion® 117 membrane, at  $125^\circ\text{C}$  for 10 min under a pressure of  $100\text{ kgf cm}^{-2}$ . The temperature set for glycerol and ethanol in the fuel cell was  $90^\circ\text{C}$  and  $80^\circ\text{C}$  respectively; and for the oxygen humidifier was  $80^\circ\text{C}$ . Also, glycerol plus KOH at a rate of  $2\text{ mol L}^{-1}$  or ethanol plus KOH at a rate of  $2\text{ mol L}^{-1}$  were delivered at approximately  $1\text{ mL min}^{-1}$ , and the oxygen flow was set to  $150\text{ mL min}^{-1}$ . Furthermore, a potentiostat/galvanostat PGSTAT 302N Autolab was used to obtain polarization curves.

### 3. RESULTS AND DISCUSSION

The X-ray diffraction analysis for Pt/C and PtCu/C electrocatalyst (Figure 1) showed a face-centred cubic structure for the platinum and its alloys. All the five characteristic peaks of a cubic structure were detected in (1 1 1), (2 0 0), (2 2 0), (3 1 1), and (2 2 2). A different diffraction peak was observed between  $20\text{-}25^\circ$ , which can be attributed to the plane (0 0 2) of the hexagonal structure of the

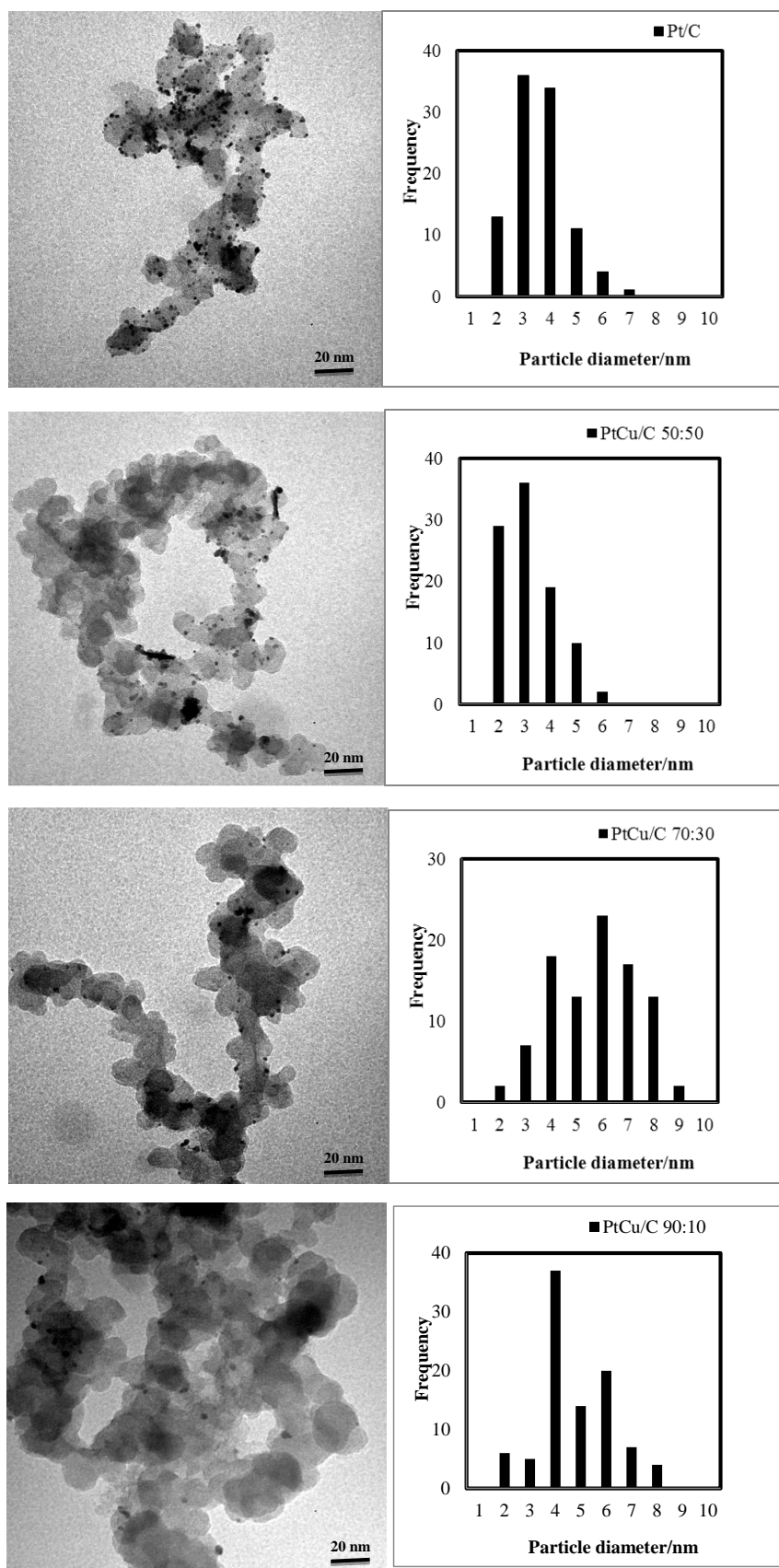
Vulcan XC72 carbon. PtCu/C electrocatalyst showed diffraction peaks located in higher values of  $2\theta$  when compared to the electrocatalyst of Pt/C. This peak location implies the formation of a solid solution between Pt and Cu, followed by the incorporation of Cu in the face-centred cubic structure of the platinum.

On the X-ray diffraction analysis for PtCu/C no peaks were detected for the presence of Cu or its oxides; nevertheless, the presence of these peaks cannot be dismissed since pure Cu or its oxides can be present in very small amount or even in an amorphous form. Cu/C usually exhibits peaks in angles of 36, 38, 42, 43, 50, 61, and 74, which correspond to the fcc structure of Cu. Furthermore, other peaks present in 36, 38, 42, and 61 can be related to the presence of Cu oxides, more specifically CuO (36, 38) and Cu<sub>2</sub>O (42, 61).



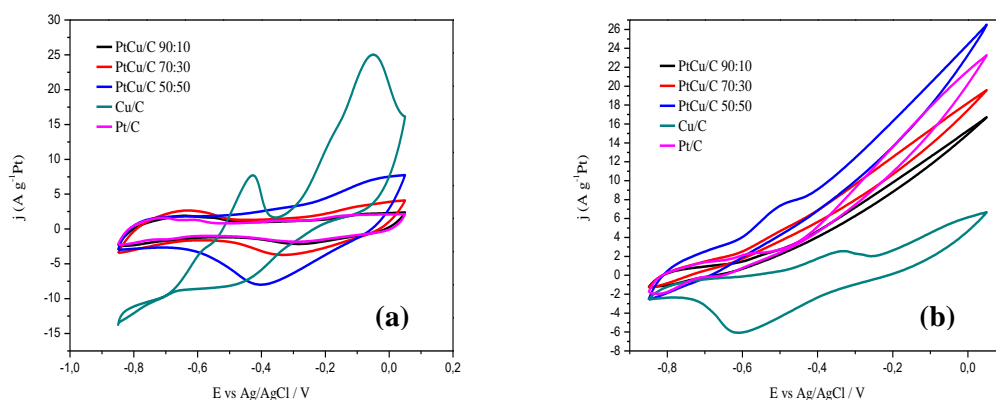
**Figure 1.** X-ray diffractograms of the Pt/C, Cu/C, and PtCu/C electrocatalysts prepared by borohydride reduction synthesis.

The micrographs obtained by TEM, presented in figure 2, for the electrocatalysts of Pt/C and PtCu/C showed nanoparticles dispersed on the carbon support. We noted for all the synthesised materials the existence of regions with clusters of particles; and this was more pronounced with the increase of copper amount on the composition of the electrocatalyst of PtCu/C. It is important to note that the nanoparticles present in the Pt/C and PtCu/C electrocatalysts have the same type of morphology.



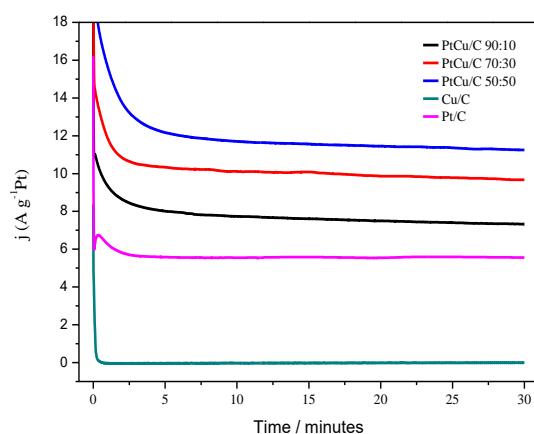
**Figure 2.** TEM images and histograms of the particle size distribution to Pt/C and PtCu/C electrocatalysts.

For the Cu/C electrocatalyst, two oxidation processes are observed on the anodic scan with the potential values: -0,4 V and 0,05 V. These processes have been attributed to the formation of copper oxides or to surfaces rich in copper. On the cathodic scan, no reduction was observed for the formed oxides suggesting that the process is irreversible or the dissolution of copper occurs. For the voltammogram of PtCu/C (Figure 3.a) we observed a region of adsorption/desorption of hydrogen (-0,85V to -0,5V) that is slightly suppressed when compared to the Pt/C electro catalyst. This behaviour is more noticeable with the increase of copper in the electrocatalyst composition. We saw that the presence of copper prevents the adsorption of hydrogen in platinum sites. On the rest of the voltammograms we also observed an increase on the current for the catalysts rich in copper, which can be attributed to a higher formation of oxygenated species on the electrocatalyst surface as recently described for other binary electrocatalysts [20, 21]. In the cathodic scan for the PtCu/C electrocatalysts prepared by the method of reduction via sodium borohydride (sodium borohydride reduction method), we observed the reduction of the oxides formed during the anodic scan. The Cu/C electrocatalyst is the less active for the oxidation of glycerol in alkaline medium when in comparison with Pt/C and PtCu/C (Figure 3.b). Nevertheless, it is important to notice that the Cu/C electrocatalyst presents some activity towards the glycerol oxidation. The PtCu/C (50:50) and PtCu/C (70:30) electrocatalysts present an initial glycerol oxidation with lower potential values when compared to the Pt/C electrocatalyst. This result, proves the beneficial effect of the addition of copper to the platinum electrocatalyst, which can be explained by the bifunctional mechanism, where the adsorption of glycerol occurs on platinum sites, while copper provides oxygenated species that facilitate the oxidation of the adsorbed intermediates on platinum, ending in the releasing the platinum site for new glycerol adsorption. The electronic mechanism cannot be discarded because the formation of alloys between Pt and Cu occurs. The PtCu/C (50:50) electrocatalyst was the most active in all the range of potential studied, especially when compared to the PtCu/C and Pt/C electrocatalyst.



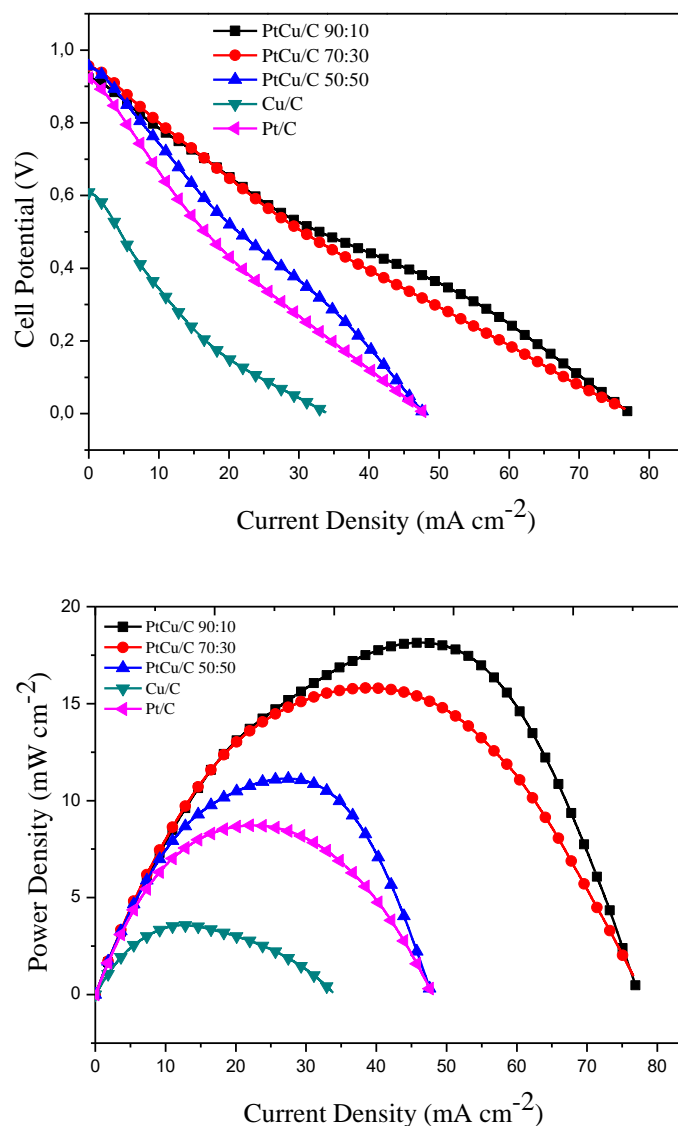
**Figure 3.** Cyclic voltammograms of Pt/C, Cu/C and PtCu/C electrocatalysts **(a)** in 1 mol L<sup>-1</sup> KOH solution; **(b)** in 1 mol L<sup>-1</sup> glycerol solution in 1 mol L<sup>-1</sup> KOH with a scan rate of 10 mV s<sup>-1</sup> at 25°C.

Figure 4 presents the chronoamperometry results for glycerol, obtained at the  $-0.4$  V potential during 1800 seconds, which show that all PtCu/C electrocatalysts were more effective for the oxidation of glycerol specially when compared to Pt/C. It is important to note that the PtCu/C (50:50) electrocatalyst presented current values two times higher than those obtained for Pt/C. These results also showed the following decreasing order of activity: PtCu/C (50:50) > PtCu/C (70:30) > PtCu/C (90:10) > Pt/C > Cu/C. Another important factor to be mentioned is that, despite the low current values presented for the Cu/C system, it presents some activity for the oxidation of glycerol in alkaline medium, as previously observed in cyclic voltammetry results. The best performance observed for PtCu/C, when compared to Pt/C, can be associated with the simultaneous occurrence of the bifunctional mechanism and the electronic effect.



**Figure 4.** Chronoamperometry curves at  $-0.4$  V in  $1 \text{ mol L}^{-1}$  glycerol solution in  $1 \text{ mol L}^{-1}$  KOH for Pt/C, Cu/C and PtCu/C electrocatalysts at  $25$  °C.

The tests on fuel cells directly fed with glycerol confirm what was observed in the electrochemical studies: 1) the PtCu/C electrocatalysts were more efficient than the Pt/C and 2) the Cu/C electrocatalyst presents an apparent activity for the oxidation of glycerol in alkaline medium (Fig. 5 a, b). In the fuel cell studies the following decreasing order of activity was observed: PtCu/C (90:10) > PtCu/C (70:30) > PtCu/C (50:50) > Pt/C > Cu/C. It is important to emphasize that the inversion of activity observed for PtCu/C is more associated to the type of normalization used in this work. When normalized by grams of platinum, the electrodes will have different thicknesses in the catalytic/diffusion layer, which implies that: the higher the amount of the second metal, the higher the thickness of the catalytic/diffuser layer will be. Consequently, the diffusion effects will be very pronounced which often mask the actual activity. However, when considering the open circuit potential, the activation region follows the same order observed in the electrochemical testes: PtCu/C (50:50) > PtCu/C (70:30) > PtCu/C (90:10) > Pt/C > Cu/C.



**Figure 5.** Curves and the power density at 90 °C of a 5 cm<sup>2</sup> direct glycerol fuel cell using Pt/C, Cu/C and PtCu/C electrocatalysts anodes (1 mg metal cm<sup>-2</sup> catalyst loading) and Pt/C E-TEK electrocatalyst cathode (1 mgPt cm<sup>-2</sup> catalyst loading with 20 wt% Pt loading on carbon), Nafion\_117 membrane KOH treated, glycerol (2.0 mol L<sup>-1</sup>) and oxygen pressure (2 bar).

The cyclic voltammograms obtained in the presence of ethanol (Figure 6 a,b) showed that all PtCu/C electrocatalysts prepared by the sodium borohydride reduction method were more effective for the oxidation of ethanol than the Pt/C electrocatalyst, while Cu/C was almost inactive for the oxidation of ethanol. The beginning of the ethanol oxidation for PtCu/C (70:30) and PtCu/C (50:50) occurs around -0.75 V, whereas for Pt/C it occurs around -0.6 V. These results show that the ethanol oxidation is favoured when a higher amount of Cu was added to the Pt electrocatalyst composition. Regarding the activity, the occurrence of the bifunctional mechanism and the electronic effect are noticeable. For the PtCu/C (90:10) electrocatalyst, the oxidation started around -0.7V. Also, for all range of potentials studied, all PtCu/C systems were more active than Pt/C systems, demonstrating their efficiency for use in ethanol fuel cell studies.



Huang [22] showed that the PtCu/C electrocatalyst had the starting point of the ethanol oxidation at values of potential less positive when compared to Pt/C. These authors concluded that the increased performance of these electrocatalysts can be attributed to superficial defects, geometric effects as well as an electronic effect on the platinum surface caused by the presence of copper. Ammam and Easton [12] also showed that the oxidation of ethanol occurs with lower potential values for PtCu/C when compared to Pt/C, and that PtCu/C also presented higher current values across the entire potential range studied. Both mentioned studies were performed in acid media, however, the authors considered that future studies are necessary regarding the use of these systems in fuel cells directly fed with ethanol.

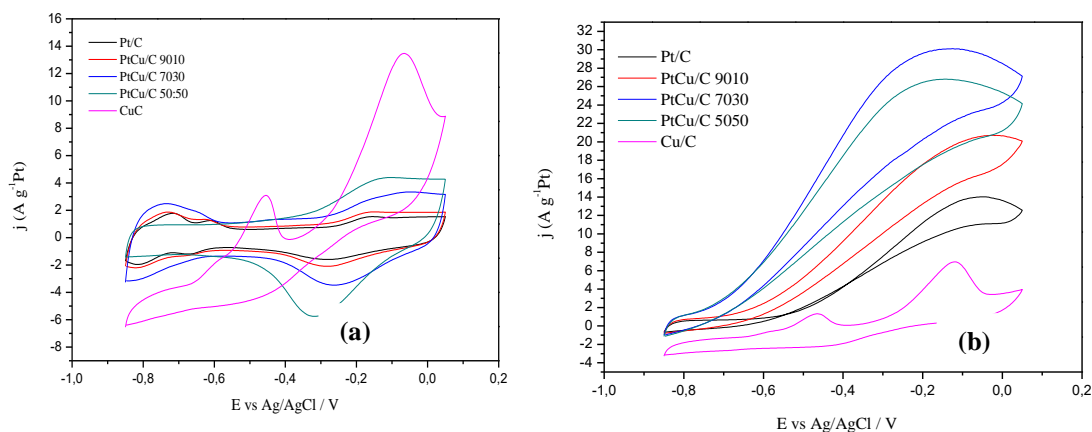


**Figure 6.** Cyclic voltammograms of Pt/C, Cu/C and PtCu/C electrocatalysts (a) in 1 mol L<sup>-1</sup> KOH solution; (b) in 1 mol L<sup>-1</sup> ethanol solution in 1 mol L<sup>-1</sup> KOH with a scan rate of 10 mV s<sup>-1</sup> at 25°C.

The results of chronoamperometry (Figure 7) obtained at the potency values of -0,4 V for 1800 seconds for the oxidation of ethanol, confirmed that all PtCu/C electrocatalysts were more effective than the Pt/C system, while Cu/C was inactive for the ethanol oxidation in alkaline medium. The results for the ethanol oxidation in alkaline medium showed the following activity after 1800 seconds: PtCu/C (70:30) > PtCu/C (50:50) > PtCu/C (90:10) > Pt/C > Cu/C. The chronoamperometry results also showed that for PtCu/C (70:30) the current values were 12 folds higher than those obtained for Pt/C, allowing us to conclude these electrocatalysts are promising for the tests with fuel cells directly fed with ethanol.

The tests in fuel cells directly fed with ethanol showed that the PtCu/C (90:10) electrocatalyst were more effective for the ethanol oxidation when compared to the Pt/C (Figure 8). Meanwhile, the Cu/c electrocatalyst presented an activity for the ethanol oxidation in alkaline medium. On the studies made with fuel cells the following activity order was observed: PtCu/C (90:10) > Pt/C ~ PtCu/C (70:30) > PtCu/C (50:50) > Cu/C.

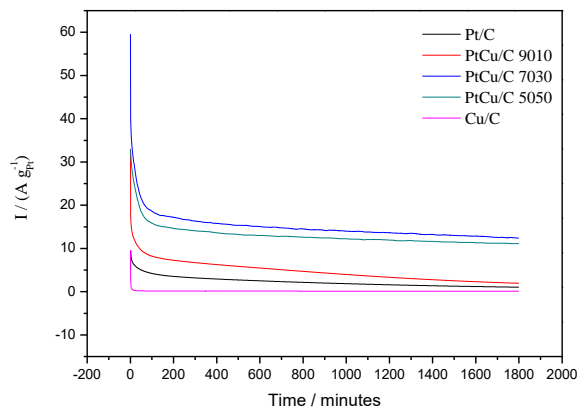


**Figure 7.** Chronoamperometry curves at -0.4 V in 1 mol L<sup>-1</sup> ethanol solution in 1 mol L<sup>-1</sup> KOH for Pt/C, Cu/C and PtCu/C electrocatalysts at 25 °C.

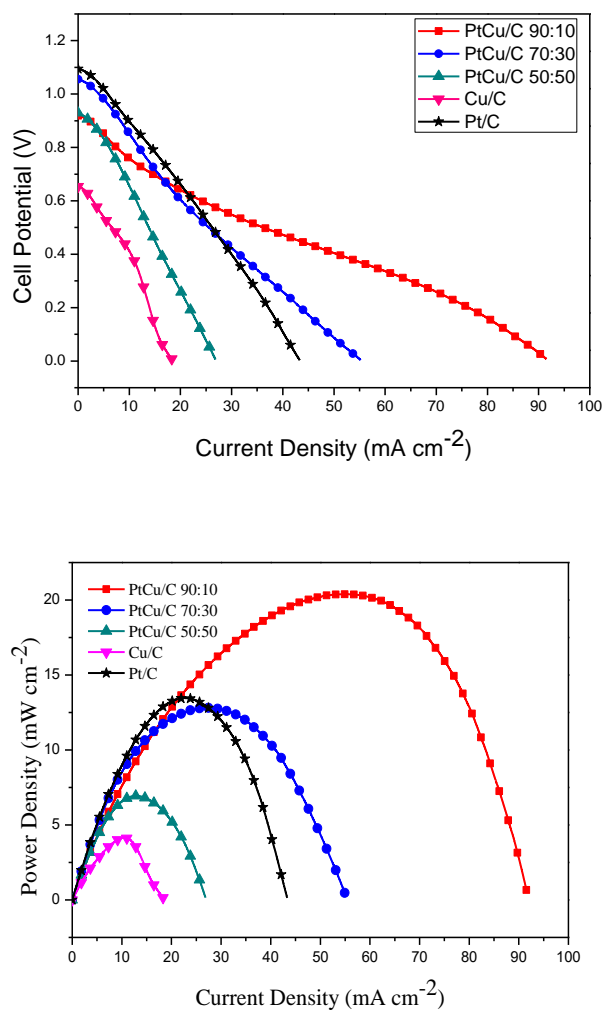


**Figure 8.** Curves and the power density at 80 °C of a 5 cm<sup>2</sup> direct ethanol fuel cell using Pt/C, Cu/C and PtCu/C electrocatalysts anodes (1 mg metal cm<sup>-2</sup> catalyst loading) and Pt/C E-TEK electrocatalyst cathode (1 mgPt cm<sup>-2</sup> catalyst loading with 20 wt% Pt loading on carbon), Nafion\_117 membrane KOH treated, ethanol (1.0 mol L<sup>-1</sup>) and oxygen pressure (2 bar).

It is important to note that the inversion of activity observed for PtCu/C is more associated to the type of normalisation used in this work. When normalisation is done per platinum grams we obtain electrodes with different thicknesses on the catalytic/diffusor layer. So the higher the amount of second metal, the higher the thickness of the catalytic/diffusor layer. As a consequence, accentuated diffusional effects will be observed which can mask the real activity. Nevertheless, the results obtained with fuel cells directly fed with ethanol also showed that the operating conditions of the cell (e.g. MEAS construction), still need to be optimised in order to obtain higher values of potency density.

#### 4. CONCLUSION

The borohydride reduction method was an efficient method to produce Pt/C and PtCu/C electrocatalysts for glycerol and ethanol electro-oxidation. The synthesized PtCu/C electrocatalysts showed the presence of PtCu (fcc) alloys. The electrochemical measurements and the experiments for both fuels, glycerol and ethanol, in DGFC and DEFC PtCu/C (90:10) presented the highest catalytic activity that can be attributed to the synergy between the constituents of the electrocatalyst. Further work is now necessary to investigate the electrocatalyst surface and to elucidate the mechanism of formic acid electro-oxidation using these electrocatalysts.

#### ACKNOWLEDGEMENTS

The authors thank the Laboratório de Microscopia do Centro de Ciências e Tecnologia de Materiais (CCTM) for the TEM measurements.

#### References

1. Q. Lin, Y. Wei, W. Liu, Y. Yu, J. Hu, *Int. J. Hydrogen Energy.*, 42 (2017) 1403.
2. F. Fathirad, A. Mostafavi, D. Afzali, *Int. J. Hydrogen Energy.*, 42 (2017) 3215.
3. Q. He, Y. Shen, K. Xiao, J. Xi, X. Qiu, *Int. J. Hydrogen Energy.*, 41 (2016) 20709.
4. A. Serov, T. Asset, M. Padilla, I. Matanovi, U. Martinez, A. Roy, K. Artyushkova, M. Chatenet, F. Maillard, D. Bayer, C. Cremers, P. Atanassov, *Appl. Catal. B: Environ.*, 191 (2016) 76.
5. C-L. Sun, J-S. Tang, N. Brazeau, J-J. Wu, S. Ntais, C-W. Yin, H-L. Chou, E.A. Baranova, *Electrochim. Acta.*, 162 (2015) 282.
6. C.A. Ottoni, S.G da Silva, R.F.B. Souza, A. O. Neto, *Electrocatalysis.*, 7 (2016) 22.
7. A.T. Marshall, V. Golovko, D. Padayachee, *Electrochim. Acta.*, 15 (2015) 370.
8. H. Rostami, A. Omrani, A. A. Rostami, *Int. J. Hydrogen Energy.*, 40 (2015) 9444.
9. J. Maya-Cornejo, N. Arjona, M. Guerra-Balcázar, L. Álvarez-Contreras, J. Ledesma- García, L.G. Arriaga, *Proc. Chem.*, 12 (2014) 19.
10. O.O. Fashedemi, K. I. Ozoemena, *Electrochim. Acta.*, 128 (2014) 279.
11. P. Mukherjee, P. S. Roy, K. Mandal, D. Bhattacharjee, S. Dasgupta, S.K. Bhattacharya, *Electrochim. Acta.*, 154 (2015) 447.
12. M. Ammam, E. B. Easton, *J. Power Sources.*, 222 (2013) 79.
13. Y. Huang, T. Zhao, L. Zeng, P. Tan, J. Xu, *Electrochim. Acta.*, 190 (2016) 956.
14. F. Li, Y. Guo, M. Chen, H. Qiu, X. Sun, W. Wang, Y. Liu, J. Gao, *Int. J. Hydrogen Energy.*, 38 (2013) 14242.
15. B. Rezaei, S. Saeidi-Boroujeni, E. Havakeshian, A.A. Ensafi, *Electrochim. Acta.*, 203 (2016) 41.

16. F. Munoz, C. Hua, T. Kwong, L. Tran, T. Q. Nguyen, J.L. Haan, *Appl Catal B: Environ.*, 174 (2015) 323.
17. E.H. Fontes, R.M. Piasentin, J.M.S. Ayoub, J.C.M. da Silva, M.H.M.T. Assumpção, E.V. Spinacé, A.O. Neto, R.F.B. De Souza, *Mater. Renew. Sustain. Energy.*, 4 (2015) 1.
18. A.O. Neto, J. Nandenha, R.F.B. De Souza, G.S. Buzzo, J.C.M. Silva, E.V. Spinacé, M.H.M.T. Assumpção, *J. Fuel Chem. Technol.*, 42 (2014) 851.
19. C.A. Ottoni, C.E.D. Ramos, S.G da Silva, E.V. Spinacé, R.F. B Souza, A.O. Neto, *Electroanalysis.*, 28 (2016) 2552.
20. H. Rostami, A. Ali, R. Abdollah, *Electrochim. Acta.*, 194 (2016) 431.
21. R.G.C.S. dos Reis, F. Colmati, *J. Solid State Electrochem.*, 20 (2016) 2559.
22. M. Huang, Y. Jiang, C. Jin, J. Ren, Z. Zhou, L. Guan, *Electrochim. Acta.*, 125 (2014) 29.

© 2018 The Authors. Published by ESG ([www.electrochemsci.org](http://www.electrochemsci.org)). This article is an open access article distributed under the terms and conditions of the Creative Commons Attribution license (<http://creativecommons.org/licenses/by/4.0/>).